A new polarised hot filament chemical vapor deposition process for homogeneous diamond nucleation on Si(100)

Costel Sorin Cojocaru, Madjid Larijani, D. S. Misra, Manoj K. Singh, Pavel Veis, Francois Le Normand

Diamond and Related Materials
13 (2004) 270–276
doi:10.1016/j.diamond.2003.10.076

A new polarised hot filament chemical vapor deposition process for homogeneous diamond nucleation on Si(100)

C.S. Cojocaru[a], M. Larijani[a], D.S.Misra[b], M.K.Singh[b], P. Veis[c], F. Le Normand[a,]

[a]*Groupe Surfaces-Interfaces, IPCMS, UMR 7504 CNRS, BP 43, 67038 Strasbourg Cedex 2, France*
[b]*Institute of Physics, Indian Institute of Technology (IIT), Powai, 400076 Mumbai, India*
[c]*Faculty of Mathematics, Physics and Informatics, Department of Plasma Physics, Comenius University, Mlynska dol. F2, 84248 Bratislava, Slovakia*

ABSTRACT: A new hot filament chemical vapor deposition with direct current plasma assistance (DC HFCVD) chamber has been designed for an intense nucleation and subsequent growth of diamond films on Si(100).Growth process as well as the *If*(*V*) characteristics of the DC discharge are reported. Gas phase constituents activation was obtained by a stable glow discharge between two grid electrodes coupled with two sets of parallel hot filaments settled in-between and polarised at the corresponding plasma potential. The sample is negatively biased with a small 10–15 V extraction potential with respect to the cathode grid.Such design allows to create a high density of both ions and radicals that are extracted and focussed onto the surface of the sample.The current density onto the sample can be finely tuned independently of the primary plasma.A homogeneous plasma fully covering the sample surface is visualized. Consequently, a high-density nucleation ($>10^{10}$ cm^{-2}) occurs.

Keywords: Diamond; HFCVD; Nucleation; Bias-enhanced HFCVD; Silicon

1. Introduction

Since the first successful report of diamond growth by the chemical vapor deposition (CVD) technique in the early 1980s [1–3], the growth of heteroepitaxial or fibre textured films [4,5] is one of the main challenges to manage the outstanding properties of diamond.Tackling such a problem requires, however, to get a high nucleation density as well as an orientation of these nuclei on the heterosubstrate.Local epitaxial orientation or fibre textured diamond films were successfully grown on silicon substrates since approximately 10 years by introducing a bias nucleation step in the microwave-assisted chemical vapor deposition (MWCVD) process [6–8].Hence, the bombardment of positively charged carbon species onto the surface was claimed to enhance diamond nucleation, although the true mechanism was far from being fully understood.By contrast, a similar bias-enhanced step introduced in the hot filament chemical vapor deposition (HFCVD) process reveals many problems that are presently neither fully understood nor experimentally well-resolved [9–26].Instead of the MWCVD process, the HFCVD process is, however, a potential alternative to grow heteroepitaxial diamond films as it can be more easily scaled up and it is by far less expensive.In fact both the ignition and the sustainance of a stable glow discharge are facilitated in the presence of hot filaments that act as an effective source of electron emission, thus enhancing the ionisation through electron collisions with the gaseous molecules or radicals activated by the hot filaments.It has been proposed that electron emission can also occur from the intense secondary emission of diamond-coated substrate holder [8,11].However, electron emission can also occur directly from the heated tungsten filaments in the HFCVD process, when the filaments were not used as anodes [13].Moreover, the role of hydrocarbon ions as active species in the diamond nucleation has been addressed: either selective etching of the non-diamond species, formation of subplanted diamond clusters or enhanced surface diffusion were proposed as possible explanations of diamond nucleation [15].In addition,

.

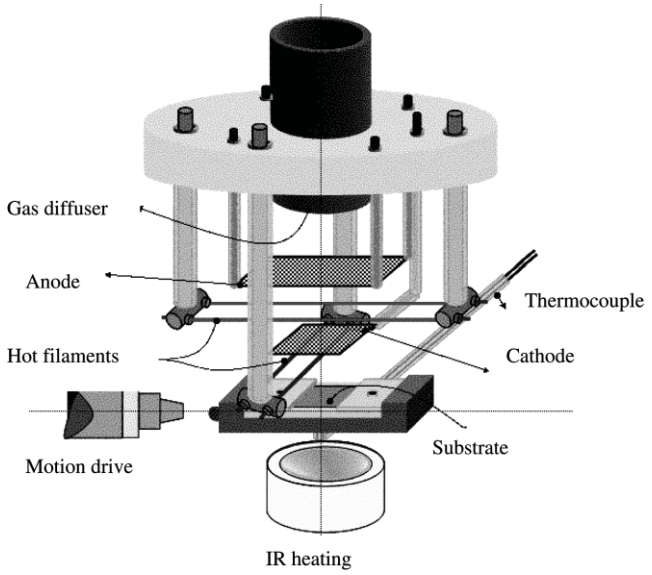

Fig.1. Scheme of the configuration electrodes–filaments–substrate.

the ionic bombardment of the surface can be highly detrimental to the quality of diamond and the rugosity of the film [12,16].Finally, due to the different nature of the substrate holder and the complex nature of the sample surface during the nucleation, the electric field may be spatially variable and time-dependent, leading to inhomogeneity and irreproducibility of the nucleation process [27–29].In this paper, a new CVD set-up has been designed to investigate the nucleation of diamond films.Details of this CVD process as well as first electrical measurements are reported.

2. Experimental part

2.1. Sample preparation

The samples were prepared in a bakeable ultra high vacuum stainless steel chamber that had been previously described in detail [30–32].The base vacuum was 10^{-9} mbar.The sample was first introduced into the preparation chamber through a motion drive.Therefore, cleaning procedures of the walls of the chamber as well as filaments carburation could be performed in the absence of the sample.The CVD deposition experiments were carried out with the same orthogonal sets of two parallel tungsten filaments (7 mm apart; diameter of 0.15 mm) and separated by 12 mm. Two electrodes both consisting in a molybdenum grid (open surface 68%) were fixed on the same moveable ensemble including the filaments (Fig.1).The anode in the form of a square grid (size 20×20 mm^2) was settled at 6 mm above the top couple of parallel filaments.The cathode grid (size 15×15 mm^2) was positioned in-between the top and the bottom couples of filaments at equal distance (6 mm).The substrate holder mounted on the motion drive was made up of an insulator ceramic MACORM, which was partially hollowed out in the center and filled with a molybdenum foil (200-mm thickness) to allow electrical contact on the rear of the substrate.The ceramic substrate holder was thoroughly cleaned before each run using SiC abrasives in order to remove the carbonaceous deposits that might initiate side electrical discharges, and subsequently ultrasonically rinsed 5 min into acetone and ethanol.The sample [Si(1 0 0) sample P-doped at 1–3 V cm; size $9\times7\times0.5$ mm^3, covered with a layer of SiO_2 (thickness 8 nm)] was strongly clamped against the molybdenum foil with isolated tungsten springs.A chromel–alumel thermocouple, handled from outside, contacted the Mo foil and was used for temperature measurement and thermal regulation during growth step and acted as electric contact for sample negative biasing during the etching and nucleation steps.The two electrodes, the filaments and the sample, were biased according to the electrical scheme sketched in Fig. 2. The variable resistances R_g, R_p, R_e as well as the fixed resistances R_1 and R_2 were calculated to stabilize both the DC discharge between the electrodes and to allow withdrawing a controlled current density of positively charged ionic species towards the substrate. The temperature was controlled and regulated by an independent infrared heater set on the rear side of the sample.The following procedure was followed to switch on the discharge during the nucleation step.First the gas mixture was admitted to the desired composition and the pressure was adjusted to 15 mbar.The filaments were switched onto the desired power as the discharge was easily ignited and stabilized by prior properly heating and biasing the filaments.The rheostat R_g was used to set the desired polarisation voltage V_p after the glow discharge ignition between the anode and the cathode.Further, with the R_p rheostat the V_{A-F} potential of the filaments was set so as the electron emission was compensated by the positive ions impinging the filaments (I_f 0–1.5 mA).Finally, the extraction voltage V_e and the intensity current on the sample I_e were adjusted at the desired values by adjusting the rheostats R_e and R_g, respectively. I_e and V_e values were kept constant at 1 mA and within 10–30 V, respectively. Furthermore, the potentials V_p and V_e needed to be continuously readjusted throughout the process with rheostats R_p and R_g.

Orders of magnitude of the plasma polarisation V_p and the extraction potential V_e were 170–200 V and 10–30 V, respectively, and the discharge current I_p was 40–100 mA, depending on the experimental conditions, but also on the cleanness of the chamber (substrate holders, walls, filaments).The extraction current was fixed in the range 1–5 mA corresponding to a current density within 1.5–7.5 mA cm^{-2}. The substrate temperature during the nucleation step T_N was monitored with an optical monochromatic pyrometer and it was checked

that the temperature rise during the nucleation step, due to the low extraction current density, did not exceed 10 K. The temperature of the filaments T_F was measured with an optical bichromatic pyrometer. The following sequences were carried out in a given deposition experiment:

- The sample was heated up to 923 K at a rate of 15 K min^{-1} under H_2 atmosphere.
- An etching procedure with a H_2 plasma for 2 min at 1023 K was achieved. The extraction current I_e was then 0.2 mA.
- The carbon was then admitted for the nucleation step, I_e and V_e were adjusted to the desired values as described above.
- At the end of the nucleation step, the polarisation and extraction potentials V_p and V_e were switched off, the CVD parameters were readjusted to the desired growth conditions (pressure P, temperature T, methane concentration C).
- The growth was finally stopped by first switching off the filament, then by stopping the carbon feed and finally by dropping the temperature (15 K min^{-1}) under hydrogen.

The experimental parameters involved in the subsequent etching, nucleation and growth steps are included in Table 1.

Table 1
Parameters of the etching, nucleation and growth steps

Step	Etching	Nucleation	Growth
T (K)	973	973	1123
CH_4 (%)	0	2–4	1
D (sccm)	100	100	200
p (mbar)	15	15	30
t (min)	2	15	60
$P_{Filaments}$ (W)	150	150	185
T_F (K)	2173	2173	2473
d_{FS}[a] (mm)	4	4	6
V_p (V)	130	(160–200)[b]	0
I_p (mA)	(5–15)[b]	(10–40)	0
V_e (V)	20	0–40	0
I_e (mA)	0.2	0.2–7	0

The variable parameters are indicated between brackets with the extension range in the nucleation process.

[a] d_{FS} is the distance between the bottom couple of filaments and the substrate (Fig.1).

[b] V_p is not an operating parameter. It depends on the quality of the diamond coating on the electrodes, the cleanliness of the walls, the substrate and filaments holders, and it might vary in the course of the process.

Preliminary to the deposition, some important operations were achieved to ensure a stable ignition of the discharge:

- If just implemented, the new filaments were carburized.

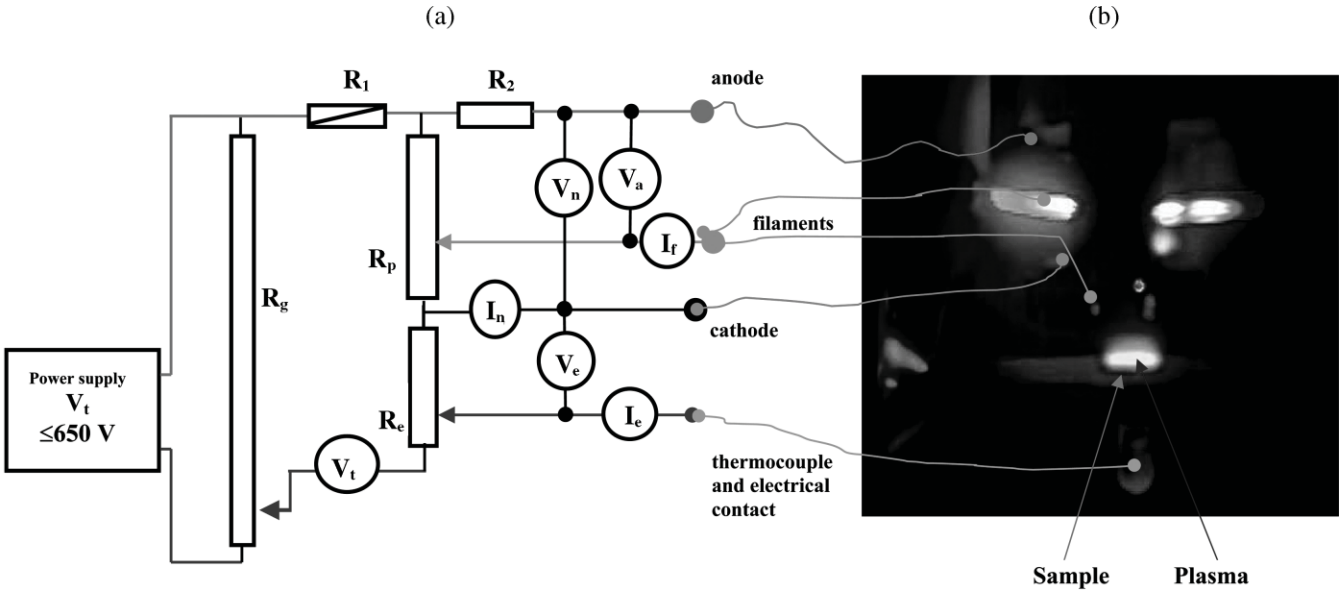

Fig.2. Electrical scheme of the polarisation process in relation to a filtered image of the discharge at the distance cathode–substrate d_{fs} 10 mm. The image of the discharge is the sum of the filtered image of H_b, CH and C_2H_2 emission lines at 486.2 nm, 431 and 518 nm, with widths 7.3; 7.4 and 8 nm and transmissions 54; 51 and 51%, respectively (Table 2). An intense blue light discharge focussed above the sample can be evidenced. The emission of the filaments on the top of the images is partly masked on the center by one pillar (Fig.1). Conditions are V_p 380 V; I_p 12.5 mA; V_e 10 V, I_e 6 mA; T 973 K; 2.5% CH_4 in H_2; P 15 mbar; T_f 2173 K. The power of the filaments and the heating lamp were dropped just before the flash.

Table 2
Observed optical emission lines and optical filters characteristics

Fragments	Emission line (nm)	Optical filters (COHERENT®)		
		Position (nm)	Width (nm)	Transmission (%)
H_a	656.2	656.3	11.58	57
H_b	486.2	488	7.28	54
CH	431.1	430	7.38	51
CH^q	417.1			
CH^q	422.2			
C_2H_2	516–520	514.5	8.00	51

– In addition to the bake out, the chamber was in situ cleaned in order to remove the carbonaceous deposits.This was carried out by a H_2 plasma between the filaments and the walls for 3 min at 30 mbar.

2.2. Sample characterization

The films were characterized by scanning electron microscopy (SEM) performed in a JEOL JSM 6700F set-up working at 10 and 3 kV, respectively.The resolution was estimated to 0.005 mm in the best case.

3. Results and discussion

A view of the discharge is shown in Fig. 2, where most of the intense radiative emission by tungsten filaments was removed just before recording the images. This image is the sum of optically filtered images of the emission line in the visible of different gas phase species H_a, H_b, CH, CH^q and C_2H_2 (Table 2).Each singly filtered image displays identical discharge (not shown).Three distinct luminescent areas can be evidenced.One of them concerns the emission around the hot filaments on top of the images. Two different glow discharges with the characteristic purple blue color are evidenced, one above the cathode and the most intense one spreading out above the sample.The discharge focussed above the sample displays intense optical emission, due to the high density of excited species generated above a small surface, which homogeneously covers the sample surface entirely.The H_b emission was more extended towards the cathode and the carbon species (CH and C_2H_2) emissions are more concentrated over the sample.These observations sustain recent numerical unidimensional simulations for electron, ions and neutral densities performed by Hash et al. [33] for a DC HFCVD reactor.Therefore, I_e can be used in the following as the true extraction current of ions impinging the surface of the sample.The high nucleation density and the homogeneity of the diamond deposit is checked after 15 min of nucleation followed by 60 min of growth (Fig.3) at three locations along the diagonal of a 9×7 mm^2 Si(1 0 0) sample.The density at the center of the sample can be estimated to approximately 10^{10} cm^{-2}. The deviation of the density is not more than 20% along the sample.The primary plasma ignited and sustained by the hot filaments is very stable.Moreover, the presence of hot filaments allows to ignitiate the plasma at voltages lower than 200 V.Further, the characteristics $I_e - f(V_e)$ as well as the influence of the plasma primary potential $I_e - f(I_p)$ were studied.These studies were performed on a Si(1 0 0) sample precovered by ECR plasma processing with a SiO_2 layer of 8-nm thickness. This surface prevents the diamond nucleation and thus avoids strong modifications of the extraction intensity I_e due to the intense secondary electron emission from diamond [34,35].

Fig.4 displays the characteristics $I_e - f(V_e)$ on SiO_2 y Si(1 0 0) at two fixed values of the primary plasma intensity I_p.Within the range of extraction potential used (0–40 V), the extraction intensity I_e increases linearly with V_e.However, the intensity as well as the slope markedly increase at higher I_p.In Fig.5 the extraction current I_e is again linearly dependent on the primary plasma intensity I_p at a fixed extraction voltage V_e.It must be noted that without any extraction voltage (V_e 0), the extraction intensity is not zero, the current density being more than 50% of the current density at V_e 20 V. Conversely, the current density clearly goes to zero when I_p decreases.

Many configurations have been introduced in the literature in order to achieve a bias step to the HFCVD process.Among these, the set-up described by Zhou et al. [25] displays some similitudes but also clear differences with the one described in this work.As in this work, a double bias was applied between an anode grid, filaments and the substrate was used as a cathode. Linear behaviours were reported both for the current extracted on the sample with the substrate bias voltage, and for the current between the anode and the filaments grid current.Moreover, large nucleation density was observed.However, the substrate voltage approximately 150 V, relative to the filaments, although decreased when compared with other set-up, remained large and it

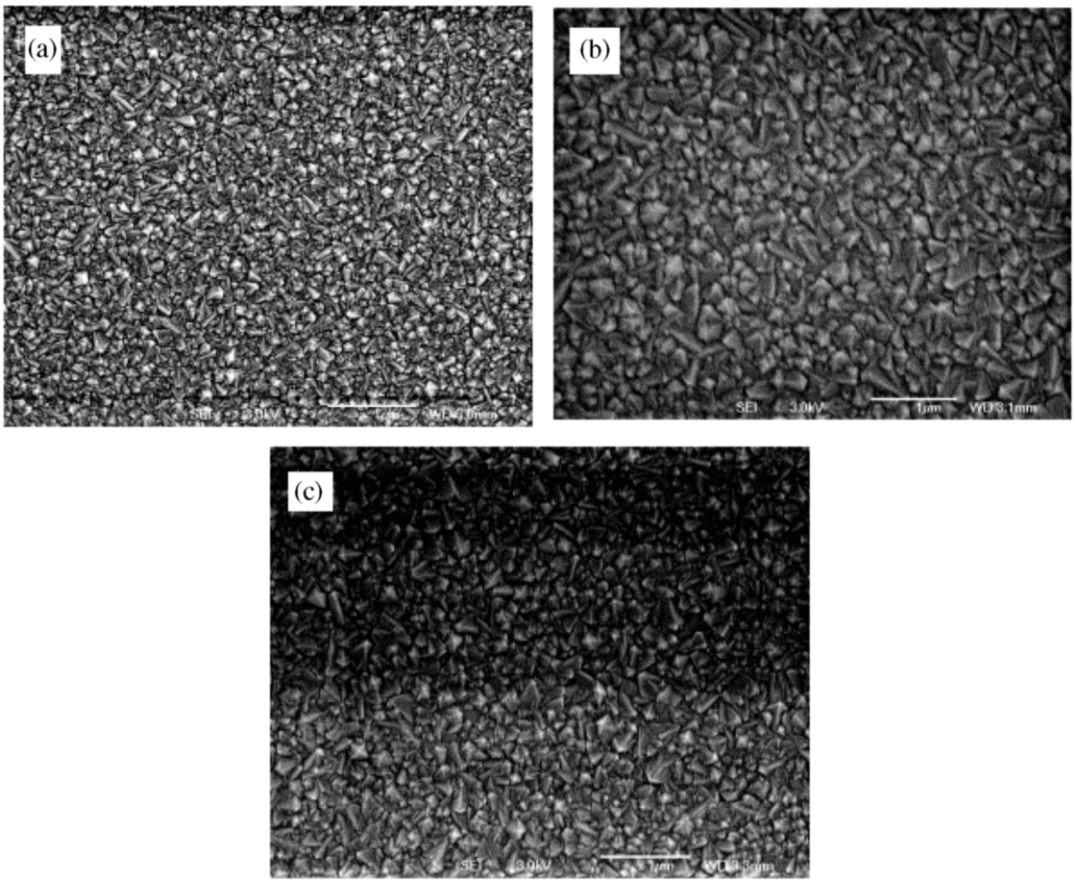

Fig.3. SEM images of a diamond deposition after 15 min nucleation and subsequent 60 min growth along the diagonal of the Si(1 0 0) sample at (a) 1 mm; (b) 6 mm and (c) 11 mm from one corner.

was expected that the energy of the ionised carbon precursors is high and led to a rapid degradation of the diamond nuclei.Reversely, in the set-up described in this work, by introducing a set of electrodes distinct from the sample a primary plasma is created with characteristics which are independent from the surface of the substrate.The introduction of a small negative extraction voltage between the cathode of the primary

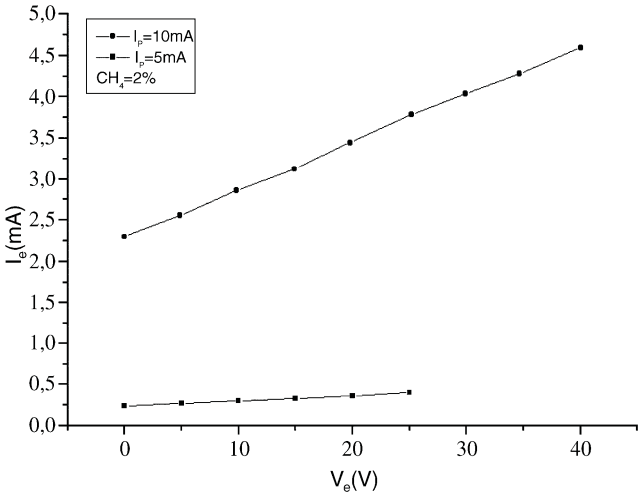

Fig.4. Characteristic $I_e \backsim f(V_e)$ of the extraction discharge for (square) $I_p \backsim 5$ mA; (circle) $I_p \backsim 10$ mA.Conditions are: $CH_4 \backsim 2\%$; substrate SiO_2ySi(1 0 0).

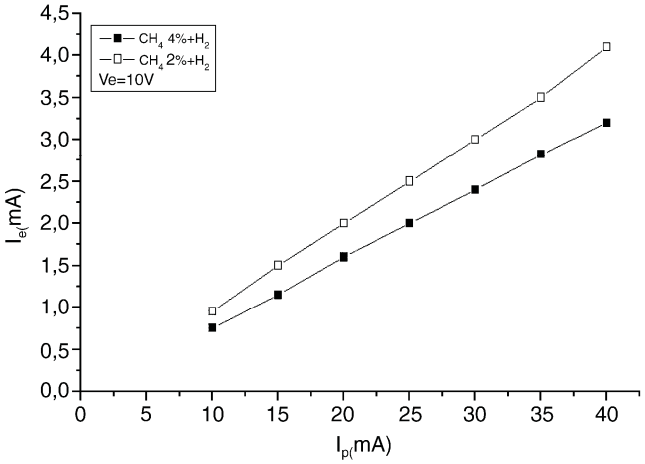

Fig.5. Plot $I_e \backsim f(I_p)$. $V_e \backsim 10$ V, (empty square) $CH_4 \backsim 2\%$; (full square) $CH_4 \backsim 4\%$; substrate SiO_2ySi(1 0 0).

plasma and the substrate allows to draw part of these ionized carbon species and to impinge the surface of the sample with a lower kinetic energy, as expected from the many collisions occurring in the discharge above the sample.This behaviour has been confirmed for different gas compositions and for different activation or geometrical parameters [35].Moreover, the filaments are maintained in our case at the potential of the plasma and therefore the emission of electrons by filaments is controlled.If not the case, the plasma becomes rapidly unstable.Now the linear behaviour of the current density on the sample with both the extraction voltage and the primary plasma intensity can be explained as follows.In the former case the extraction discharge above the sample acts as a resistive column through the many collisions occurring in this region.In the latter case, many ionic species accelerated in the primary plasma towards the open grid cathode cross it and are collected by the discharge established between the cathode and the sample, which is slightly negatively biased relative to this cathode.This is supported by the detection of a significant current density on the sample, even when no extraction voltage has been applied.

Of course in this rather complex system the properties of the ionic carbon species (mean and distribution of kinetic energy, density, nature) will depend both on the electrical parameters of the two discharge generated and on the geometric configuration, especially the distance between the cathode and the substrate [33,35], in addition to the parameters of the HFCVD process.It is especially expected to get with this set-up a narrow and controlled distribution of the kinetic energy of the carbon ions precursor of the diamond nucleation, and therefore to achieve a control of this important step.Further works are done in this direction.

4. Conclusion

A new DC HFCVD chamber has been designed for an intense nucleation and subsequent growth of diamond films on Si(1 0 0).In a DC discharge and hot filaments-assisted nucleation step, the activation of the gas phase was obtained through a stable primary plasma created between polarised electrodes approximately 180 V with a couple of two parallel filaments settled in-between and set at the plasma potential.In addition, a second and small extraction discharge of 10–15 V is introduced between the cathode and the sample, negatively charged. Such design allows to create a high density of both ions and radicals that are extracted and focussed onto the surface of the sample.The characteristics of the current density onto the sample can be finely tuned as a function of the primary plasma intensity or the extraction voltage drop.By qualitative optical emission analysis, preferential localization of the carbon-activated species is observed above the substrate confirming numerical simulations on a DC HFCVD reactor [33].Further 1-h growth by a classical diamond HFCVD process yields diamond films that are characterized by SEM.Large density and high homogeneity over an area approximately 9.7 mm^2 have been found. It is expected that such a process will lead to a more accurate control of the nucleation step with a high density and a high reproducibility.

Acknowledgments

Fruitful discussions with C.Fuchs (PHASE, Strasbourg, France) are greatly appreciated.J.Faerber (IPCMSyGSI, Strasbourg, France) for SEM observations and P.Legagneux (Thales R&D, Orsay, France) for purchasing the SiO_2ySi(1 0 0) samples are acknowledged.

References

[1] M. Kamo, Y.Sato, M. Matsumoto, N.Setaka, J. Cryst. Growth 62 (1983) 642.
[2] J.C. Angus, C.C. Hayman, Science 241 (1988) 913.
[3] W.A. Yarbrough, R. Messier, Science 247 (1990) 688.
[4] S.T. Lee, Z.Lin, X.Jiang, Mater. Sci. Eng.25 (1999) 123.
[5] S.T. Lee, H.Y. Peng, X.T. Zhou, et al., Science 287 (2000) 104.
[6] S.Yugo, T.Kanai, T.Kimura, Diamond Relat. Mater. 1 (1992) 929.
[7] H. Kawarada, T.Suesada, H.Nagasawa, Appl.Phys.Lett. 66 (1995) 583.
[8] R.Stockel, K. Janischowsky, S.Rohmfeld, J.Ristein, M. Hundhausen, L.Ley, Diamond Relat. Mater. 5 (1996) 321.
[9] W.Zhu, F.R.Sivazlian, B.R.Stoner, J.T.Glass, J. Mater. Res. 10 (1995) 425.
[10] F.Stubhan, M. Ferguson, H.J.Fusser, R.J. Behm, Appl. Phys. Lett.66 (1995) 1900.
[11] Q. Chen, J.Yang, Z.Lin, Appl.Phys.Lett. 67 (1995) 1853.
[12] Q.Chen, Z.Lin, Appl.Phys. Lett.68 (1996) 2450.
[13] W.L. Wang, G. Sanchez, M.C. Polo, R.Q. Zhang, J. Esteve, Appl.Phys.A 65 (1997) 241.
[14] X.Li, Y.Hayashi, S.Nishino, Diamond Relat. Mater. 6 (1997) 1117.
[15] X.Li, Y.Hayashi, S.Nishino, Thin Solid Films 308 (1997) 163.
[16] G. Sanchez, M.C. Polo, W.L. Wang, J. Estève, Diamond Relat. Mater.7 (1998) 200.
[17] I.Gouzman, A.Hoffman, Diamond Relat. Mater.7 (1998) 209.
[18] Y.Chen, F. Chen, E.G.Wang, J. Mater. Res. 13 (1998) 126.
[19] K.J. Liao, W.L.Wang, B.Feng, Phys.Status Solidi A 167 (1998) 117.
[20] J.B. Cui, N.G. Shang, R.C. Fang, J. Appl. Phys. 83 (1998) 6072.
[21] W.L.Wang, K.J.Liao, J.Wang, et al., Diamond Relat. Mater. 8 (1999) 123.
[22] J.Esteve, M.C. Polo, G.Sanchez, Vacuum 52 (1999) 133.
[23] D.M.Li, J.Larjo, R. Hernberg, T.Mantyla, Diamond Relat. Mater.8 (1999) 1135.
[24] I.U. Hassan, C.A. Rego, N. Ali, W. Ahmed, I.P. O'Hare, Thin Solid Films 355 (1999) 134.

[25] X.T. Zhou, H.L. Lai, H.Y. Peng, et al., Diamond Relat. Mater. 9 (2000) 134.
[26] B.H. Song, D.Y. Yoon, Diamond Relat. Mater. 9 (2000) 82.
[27] B.Kulisch, L.Ackermann, B. Sobisch, Phys. Status Solidi A 154 (1996) 155.
[28] M.Schreck, B.Stritzker, Phys. Status Solidi A 154 (1996) 197.
[29] S.Barrat, S.Saada, I. Dieguez, E. Bauer-Grosse, J. Appl. Phys. 84 (1998) 1870.
[30] L.Demuynck, Thesis, University Louis Pasteur, Strasbourg, France, 1995.
[31] L.Constant, C.Speisser, F. Le Normand, Surf. Sci. 387 (1997) 28.
[32] J.C. Arnault, L. Demuynck, C.Speisser, F.Le Normand, Eur. J.Phys. Chem. B 11 (1999) 327.
[33] D. Hash, D.Bose, T.R. Govindan, M.Meyyappan, J. Appl. Phys.93 (10) (2003) 6284.
[34] G.T. Mearini, I.L. Krainsky, J.A. Dayton Jr., Surf. Interface Anal.21 (1994) 138.
[35] C.S. Cojocaru, Larijani, F. Le Normand, unpublished results.